

# BIOMECHANICS

OPEN

# Finite Element Comparison of the Spring Distraction System and the Traditional Growing Rod for the Treatment of Early Onset Scoliosis

Justin V.C. Lemans, MD,<sup>a</sup> Manoj K. Kodigudla, MS,<sup>b</sup> Amey V. Kelkar, MS,<sup>b</sup> Daksh Jayaswal, MS,<sup>b</sup> René M. Castelein, MD, PhD,<sup>a</sup> Moyo C. Kruyt, MD, PhD,<sup>a</sup> Vijay K. Goel, PhD,<sup>b</sup> and Aakash Agarwal, PhD<sup>c</sup>

**Study Design.** Finite element analysis (FEA).

**Objective.** The aim of this study was to determine biomechanical differences between traditional growing rod (TGR) and spring distraction system (SDS) treatment of early-onset scoliosis.

**Summary of Background Data.** Many "growth-friendly" implants like the TGR show high rates of implant failure, spinal stiffening, and intervertebral disc (IVD) height loss. We developed the SDS, which employs continuous, dynamic forces to mitigate these limitations. The present FEA compares TGR and SDS implantation, followed by an 18-month growth period.

**Methods.** Two representative, ligamentous, scoliotic FEA models were created for this study; one representing TGR and one representing SDS. initial implantation, and up to 18 months of physeal spinal growth were simulated. The SDS model was continuously distracted over this period; the TGR model included two additional distractions following index surgery. Outcomes included differences in rod stress, spinal morphology and iVD stress-shielding.

**Results.** Maximum postoperative von Mises stress was 249MPa for SDS, and 205MPa for TGR. During the 6-month TGR

From the <sup>a</sup>Department of Orthopedics, University Medical center Utrecht, Utrecht, The Netherlands; <sup>b</sup>Department of Bioengineering and Orthopedic Surgery, Engineering center for Orthopedic Research Excellence (E-CORE), University of Toledo, Toledo, OH; and <sup>c</sup>Spinal Balance inc, Swanton, OH. Acknowledgment date: June 21, 2021. First revision date: July 29, 2021. Acceptance date: November 12, 2021.

This is an open access article distributed under the terms of the creative commons Attribution-Non commercial-No Derivatives License 4.0 (CCBY-NC-ND), where it is permissible to download and share the work provided it is properly cited. The work cannot be changed in any way or used commercially without permission from the journal.

The device(s)/drug(s) that is/are the subject of this manuscript is/are not FDA-approved for this indication and is/are not commercially available in the United States

Stryker Spine (formerly K2 M) funds were received in support of this work. Relevant financial activities outside the submitted work: board membership, consultancy.

Address correspondence and reprint requests to Justin V.C. Lemans, MD, University Medical center Utrecht, Department of Orthopedic Surgery, P.O. Box 85500, 3508GA Utrecht, The Netherlands; E-mail: j.v.c.lemans-3@ umcutrecht.nl

DOI: 10.1097/BRS.00000000000004297

distraction, TGR rod stress increased over two-fold to a maximum stress of 417MPa, compared to a maximum of 262 MPa in the SDS model at 6-month follow-up. During subsequent follow-up periods, TGR rod stress remained consistently higher than stresses in the SDS model. Additional lengthenings in the TGR model led to a smaller residual curve (16.08) and higher T1-S1 growth (359 mm) at 18-month follow-up compared to the SDS model (26.98, 348 mm). During follow-up, there was less stress-shielding of the IVDs in the SDS model, compared to the TGR model. At 18-month follow-up, upper and lower IVD surfaces of the SDS model were loaded more in compression than their TGR counterparts (mean upper:  $\pm$ 112  $\pm$ 19N; mean lower:  $\pm$ 100  $\pm$ 17N).

**Conclusion.** In the present FEA, TGR treatment resulted in slightly larger curve correction compared to SDS, at the expense of increased IVD stress-shielding and a higher risk of rod fractures.

**Key words:** biomechanics, deformity, early onset scoliosis, finite element analysis, rod fracture, scoliosis, spring distraction system, traditional growing rod.

**Level of Evidence.** N/A **Spine 2022;47:E456-E465** 

n early-onset scoliosis (EOS), "growth-friendly" instrumentation aims to correct spinal deformities, whilst facilitating spinal and thoracic growth. Distraction-based growing rods increase spinal and thoracic length using periodic implant lengthenings. One commonly used distraction-based implant is the traditional growing rod (TGR). Its main disadvantage is the necessity for multiple lengthening surgeries. These require frequent anesthetic events (with potentially harmful neurodevelopmental effects) and increase the risk of wound complications. Although controlled growing rod (MCGR) was developed, which allows for noninvasive magnetic lengthening. Although both implants are effective at controlling the deformity, they have certain disadvantages. Both systems exhibit the

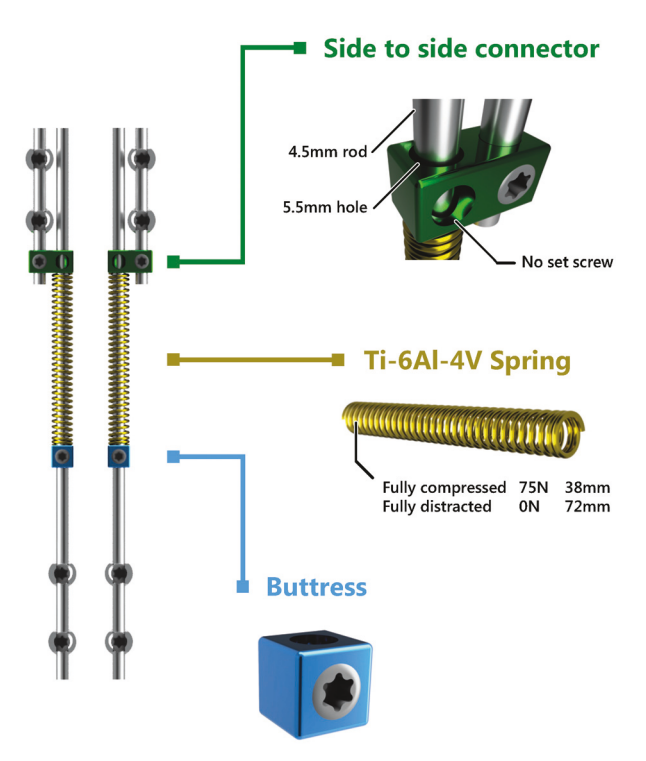


**Figure 1.** Spring Distraction System concept. The Spring Distraction System consists of two long rods (4.5 mm Co-Cr-Mo) that are able to slide through an oversized side-to-side connector (5.5 mm Ti-6Al-4 V, green). A helical spring (Ti-6Al-4 V, gold) with a maximum force of 75N is compressed against the connector proximally, and kept in a compressed state distally by a buttress (blue) that is mounted on the rod. During follow-up, the spring distracts the spine with attenuating force whilst lengthening from 38 mm (compressed) to 72 mm (uncompressed).

"law of diminishing returns," wherein later distractions do not reach the growth potential shown during earlier lengthenings. <sup>5–8</sup> In addition, implant complications such as screw pull-out, rod fractures and MCGR actuator failure are frequently observed. <sup>4,9–13</sup> Previous studies have implicated spinal stiffening and autofusion, which also necessitates higher periodic distraction forces, as a potential cause for both the "law of diminishing returns" and the high rate of implant complications. <sup>14–16</sup>

At our institution, a novel "growth-friendly" concept was developed that aims to circumvent both disadvantages by combining the strengths of both distraction-based- and guided-growth implants. This Spring Distraction System (SDS) employs helical springs to continuously distract growing rods that freely slide through open side-to-side connectors (Figure 1). The continuous SDS force application removes the need for reoperations and the dynamic coupling of the rods should allow for residual spinal motion and could prevent stress-shielding of the spine, which may lower implant stresses, and prevent intervertebral disc (IVD) height loss. 19-21 Investigating these potential advantages in vivo is difficult, especially from an ethical point of view. However, in-silico comparisons between implants that use continuous distractive forces (e.g., SDS) and those that use intermittent forces (e.g., TGR) could be a second-best

alternative. The present study aims to show differences between the SDS and TGR implants by simulating implantation and 18-month follow-up with physeal growth in a single, representative EOS finite element (FE) model. By performing two simulations, wherein everything but the used implant is kept identical, similarities and differences between the two strategies can be highlighted. The main investigated outcome is the magnitude and location of von Mises stresses (responsible for fatigue failure) in the rods during the course of treatment. Secondary outcomes are differences in spinal morphology during treatment (coronal Cobb angle, kyphosis/lordosis and T1-S1 height) and differences in IVD loading.

#### MATERIALS AND METHODS

#### **Finite Element Scoliotic Spine Model**

A ligamentous, patient-specific, scoliotic FE model was used in this study. This was done by translating the nodes of a previously created, volumetric, ligamentous healthy spinal FE model until they matched the radiographic scoliotic curve of a real EOS patient (9-year-old female, C-EOS type I2N, T9 apex), both in the coronal (Cobb 448) and the sagittal plane (T5-T12 kyphosis: 258, L1-S1 lordosis: 528). The model was validated previously and has been used in several FE studies. 15,16,22-25

### Simulation of Surgery and Follow-up Growth

After successful creation of the curve, growing rod implantation surgery was modeled in several steps (Figure 2). Pedicle screws were inserted proximally (T2-4) and distally (L1-3). Mounting of two short rods was simulated on the proximal pedicle screws and mounting of two long rods was simulated on the distal pedicle screws. The proximal and distal rods were then connected with a side-to-side connector. The spine and implants were modeled to match the postoperative radiographic shape in both the coronal and sagittal plane. Two versions of the same model were created; one that mimicked TGR (side-to-side connector fixed to both rods after each distraction, bi-annual distraction) and one that mimicked SDS (free sliding side-to-side connector and 75N spring distraction). Except for the sliding connector and the addition of the SDS springs, both models were identical with respect to pre-operative curve morphology and intraoperative implant position. The connector was fixated to both rods in the TGR model through tie interactions, whereas in the SDS model, one rod was able to slide through the oversized connector through a sliding contact interaction (hard contact, friction coefficient: 0.1). The SDS spring was modeled as an analytical spring element between the inferior face of the side-to-side connector and a prespecified point of the rod 72 mm from the cross-connector (simulating an uncompressed spring). First, displacement control was used in both models to simulate distraction of 20 mm in the preoperative model. In the TGR model, the rods were then fixed in the connector. In the SDS model, after initial distraction, the distal end of the spring was

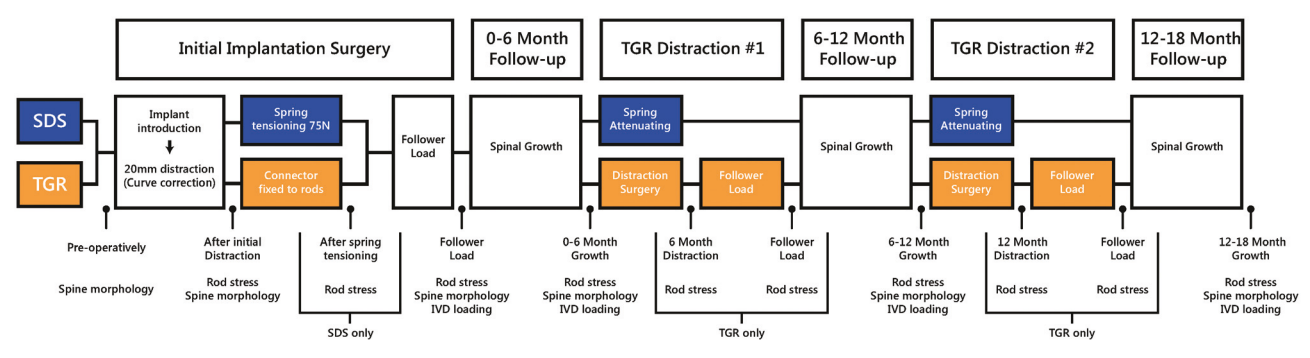


**Figure 2.** Simulation timelines with measuring points. In both models, implantation surgery and 18 months of postoperative follow-up was simulated. For the SDS model, the simulation included spring tensioning and three periods of physeal growth with attenuating spring forces. For the TGR model, additional distractions were modeled at 6- and 12-month follow-up. The timepoints where rod stress, spine morphology and intervertebral disc loading were compared can be seen in the bottom of the figure for each model. IVD indicates intervertebral disc; SDS, Spring Distraction System; TGR, traditional growing rod.

displaced along the rod (while fixing the connector position) until a predefined length of 38 mm was reached (simulating a fully compressed spring). Then, the distal end of the spring was fixed, the connector piece released and spring distraction commenced. Spring length and stiffness (k = 2.15 N/mm) were identical to the parameters used clinically. Gravity and stabilizing muscle forces (i.e., post-surgical erect ambulation) were simulated through use of a follower load, following the sagittal spinal contour. The T1 vertebra was loaded with 14% of body weight, every subsequent vertebra was loaded with an additional 2.6% of body weight. <sup>22,26</sup> In the TGR model, during each distraction, the side-to-side connectors were uncoupled from the rods, and a bilateral force (130N per rod) was applied pushing the rods apart, after which the rods were both fixed to the side-to-side connector again.

Material properties in the models were taken from the literature and were similar to values used in previously reported FE studies (Table 1).<sup>27</sup> The inferior surface of S1 was fixed in all degrees of freedom. Spinal growth was modeled using a previously employed method, in which the Hueter-Volkmann law describing physeal growth was emulated through the equation:  $G = G_m$ "[1- $\beta(\sigma - \sigma_m)$ ] (G: The actual spinal growth strain, Gm": The baseline spinal growth strain (0.035/6 months),  $\sigma$ : The actual compressive stress (MPa) on the spinal physis,  $\sigma_m$ : The baseline compressive stress (MPa) on the spinal physis,  $\beta$ : 1.5 MPa <sup>-1</sup>). <sup>28-30</sup> These values were calculated during each simulation step, after which the physeal forces were converted to growth strains. These growth changes were then divided equally over the spanned vertebral body elements of the growth plates, increasing vertebral body size.

| Material                  | Element Used                              | Young's Modulus,<br>MPa  | Poisson<br>Ratio | Other Properties  |
|---------------------------|---|--------------------------|------------------|---|
| Cortical bone             | Linear hexahedral (C3D8)                  | 75                       | 0.29             |   |
| Cancellous bone           | Linear hexahedral (C3D8)                  | 75                       | 0.29             |   |
| Posterior bone            | Linear hexahedral (C3D8)                  | 200                      | 0.25             |   |
| Annulus fibrosis (ground) | Neo-Hookean hexahedral (C3D8)             |                          |                  | C10 = 0.348<br>D1 = 0.3   |
| Annulus fibrosis (fibers) | Rebar elements                            | 357-550                  |                  |   |
| Nucleus pulposus          | Linear hexahedral (C3D8H)                 | 1                        | 0.4999           |   |
| Apophyseal joints         | Nonlinear soft contact,<br>GAPUNI element | 12,000                   |                  |   |
| Ligaments                 | Tension only truss elements (T3D2)        | 90% of adult values [27] |                  |   |
| Ti-6Al-4V                 | Linear hexahedral (C3D8)                  | 115,000                  | 0.30             |   |
| Co-Cr-Mo                  | Linear hexahedral (C3D8)                  | 210,000                  | 0.29             |   |
| Spring                    | Analytical Spring element                 |                          |                  | K = 2.15<br>Uncompressed length:<br>72 mm Compressed length:<br>38 mm |

E458 www.spinejournal.com May 2022

Design of the instrumentation was performed in Solidworks (Dassault Systémes, SolidWorks Corporation, Waltham, MA). The creation of the spine models, as well as the FE analyses were performed with Abagus CAE v6.14 (Dassault Systémes, SIMULIA, Providence, RI).

#### **Analysis and Outcomes**

In both models, we simulated distraction and physeal spinal growth until 18-month follow-up, just before (not including) the 18-month TGR distraction. The SDS continually distracts during this follow-up, where spring forces linearly decrease as they increase in length (75N at 38 mm; 0N at 72 mm). For the TGR model, two distractions after the index surgery (6- and 12-month distraction) were modeled according to current standard of care. The simulation steps and the evaluated follow-up points in the different models are shown in Figure 2. The primary outcome was von Mises stress in the rods. Maximum stress was identified in each of the four rods, excluding the interacting rod surfaces. Rod stress was compared intraoperatively, postoperatively after follower load introduction, and at 6-, 12-, and 18-month follow-up. For the TGR model, rod stresses before and after each distraction were determined. The size and location of maximum stress in every rod was evaluated and compared between both implants. Secondary outcomes were the coronal Cobb angles, T5-T12 kyphosis, L1-S1 lordosis and T1- S1 height, which were measured by measuring the length and angles between pre-specified elements across the relevant vertebral endplates. Loading of the IVD was measured for each IVD within the distraction construct (i.e., IVDs in the segment between the proximal and distal screws) by measuring compressive/tensile loads normal to the superior and inferior IVD surface using free-body diagrams. These values were graphed and compared at different time-points for both models.

#### **RESULTS**

The final FE models included 589,466 (SDS) and 609,628 (TGR) nodes and 448,918 (SDS), and 466,164 (TGR) elements, respectively. The instrumented model is shown in Figure 3A-D. To find a balance between mesh accuracy and computational efficiency, a mesh convergence (h-refinement) study was performed on the rod meshes until rod stresses between three consecutive mesh densities varied <5%. Ultimately, this resulted in a rod element size of  $\sim 0.5$  mm.

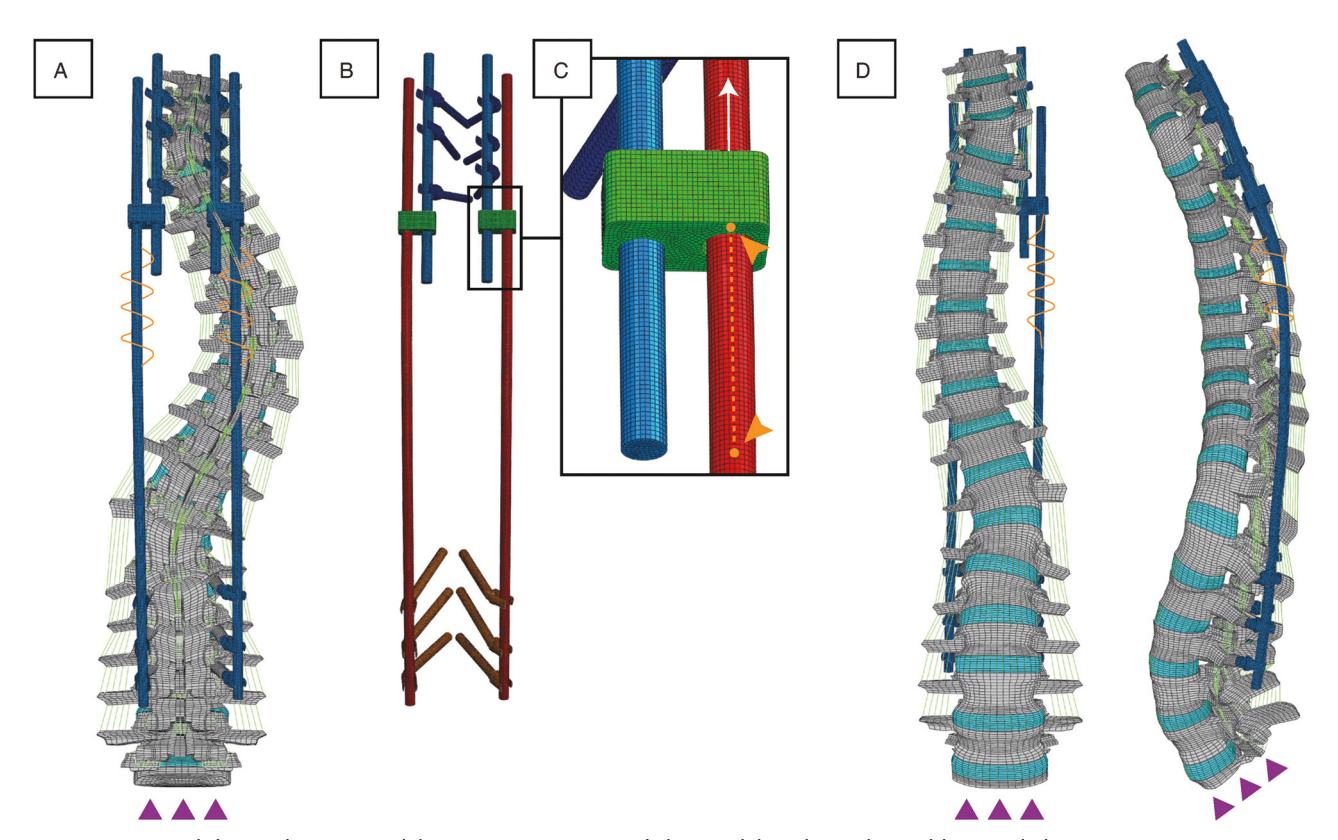


Figure 3. Instrumented finite element model. A, Posterior view of the model with implants (blue) and the SDS springs (orange). During simulation, the inferior side of S1 is fixed in all degrees of freedom (purple triangles). B, Rod and screw configuration. The proximal rods (blue) are tied to the proximal pedicle screws and to the side-to-side connector (green). The distal rods (red) are mounted on the distal pedicle screws and are either tied to the side-to-side connector (TGR) or are able to slide through it (SDS). C, The expanded view shows the sliding direction of the connector over the rod during growth (white arrow). The SDS spring is fixated on one side onto the inferior face of the sideto-side connector and on the other side onto the sliding rod after having been compressed (orange arrows). D, Anterior and sagittal view of the instrumented spine. SDS indicates Spring Distraction System; TGR, traditional growing rod.

Spine www.spinejournal.com E459

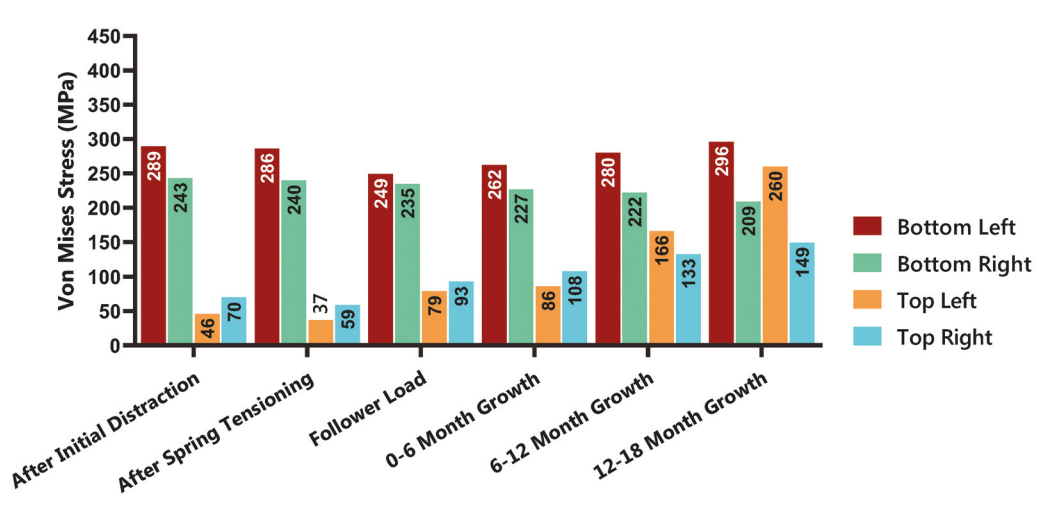


Figure 4. Spring Distraction System von Mises stress over time. Each bar denotes a different rod used in the construct. Von Mises stress in MPa

Von Mises rod stress magnitude for the different models is shown in Figure 4 (SDS) and Figure 5 (TGR). Maximum Von Mises stress postoperatively (after follower load introduction) was 249 MPa for SDS and 205 MPa for TGR. At the end of the 6-month follow-up (before the first additional TGR distraction), maximum stress in the SDS rods was 30 to 89 MPa higher compared to the respective TGR rods. However, already during the first TGR distraction at 6 months, maximum von Mises stresses in the TGR rods increased over two-fold with a maximum of 417 MPa (bottom left rod), 59% higher than the maximum SDS rod stress (262 MPa). TGR rod stresses decreased somewhat as follower load was applied, decreased further during spinal growth but increased again during the next distraction. Overall, starting at the 6-month distraction, TGR von Mises stresses remained consistently higher than those in the SDS model, where a maximum of 296 MPa was seen at the end of 18month follow-up. Stress plots with the location of increased rod stress are shown in Figure 6 (TGR) and Figure 7 (SDS). There were characteristic differences in stress location between models that were already present after the initial surgery. For the TGR model, stress maxima were consistently present in the mid-construct section of the long rods, whereas in the SDS model, stresses were distributed near the rod-screw interface. During each TGR distraction, stresses shifted towards the vicinity of the distal anchor sites; then during spinal growth, the stress maxima returned to the mid-construct of the long rods. Overall, the TGR model had larger regions of increased stress compared to the SDS model.

Secondary outcomes are shown in Table 2. The initial main coronal curve of  $43.9^{\circ}$  decreased to  $22.2^{\circ}$  (SDS) and  $23.0^{\circ}$  (TGR) postoperatively. The additional lengthenings in the TGR model led to a smaller residual curve at 18-month follow-up compared to the SDS model (SDS:  $26.9^{\circ}$ , TGR:  $16.0^{\circ}$ ). Sagittal profile was similar in both models, although the SDS was able to induce a stronger thoracic kyphosis at 18-month follow-up (SDS:  $22.7^{\circ}$ ; TGR:  $16.6^{\circ}$ ). T1-S1 height at 18-month follow-up was 347.5 mm for the SDS model compared to 359.2 mm for the TGR model.

The compressive/tensile loads on the IVDs spanned by the growing construct can be seen in Figure 8. Although the SDS model initially showed lower relative compressive forces across the superior and inferior IVD surface compared to the

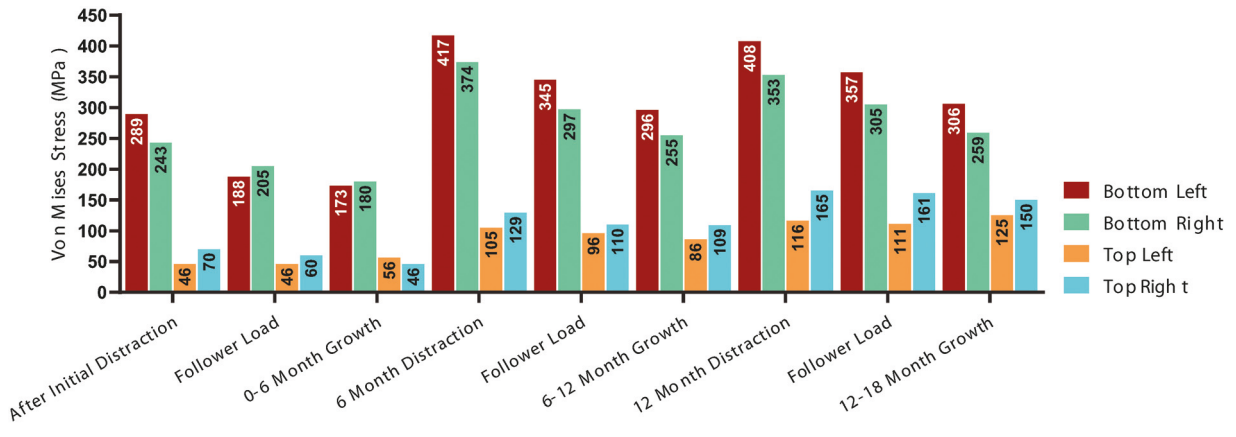
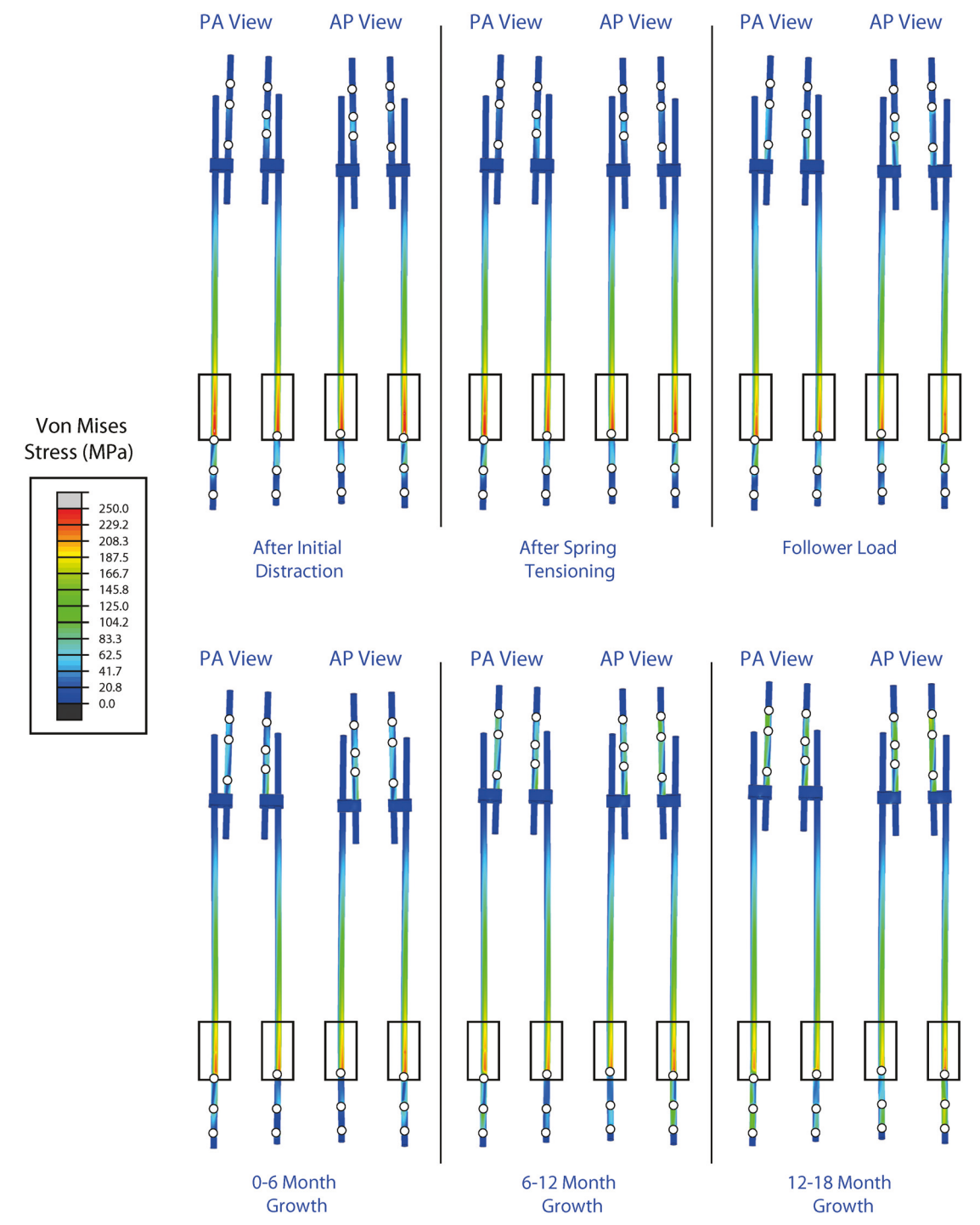


Figure 5. Traditional Growing Rod von Mises stress over time. Each bar denotes a different rod used in the construct. Von Mises stress in MPa.

E460 www.spinejournal.com May 2022



**Figure 6.** Von Mises stress plots in the Spring Distraction System model. Stress magnitude and locations in each rod are shown in the PA and AP positions. Changes over time are shown from top left to bottom right. The regions of high stress are outlined in black. AP indicates anterior-posterior; PA, posterior-anterior.

TGR model, this reversed following the TGR distraction at 6 months. At 18-month follow-up, the upper IVD surfaces in the SDS model were all under higher compressive loads (mean difference:  $+112\pm19\mathrm{N}$ ) than their TGR counterparts. For the lower IVD surfaces, the same pattern was seen with higher compressive loads in the SDS model (mean difference:  $+100\pm17\mathrm{N}$ ).

## **DISCUSSION**

The present study demonstrated characteristic differences between the TGR and SDS in a representative, EOS FE model. An important difference was the overall higher implant stresses seen during the periodic TGR lengthenings, compared to the SDS. These additional lengthenings with higher force in the TGR model resulted in additional curve

Spine www.spinejournal.com **E461** 

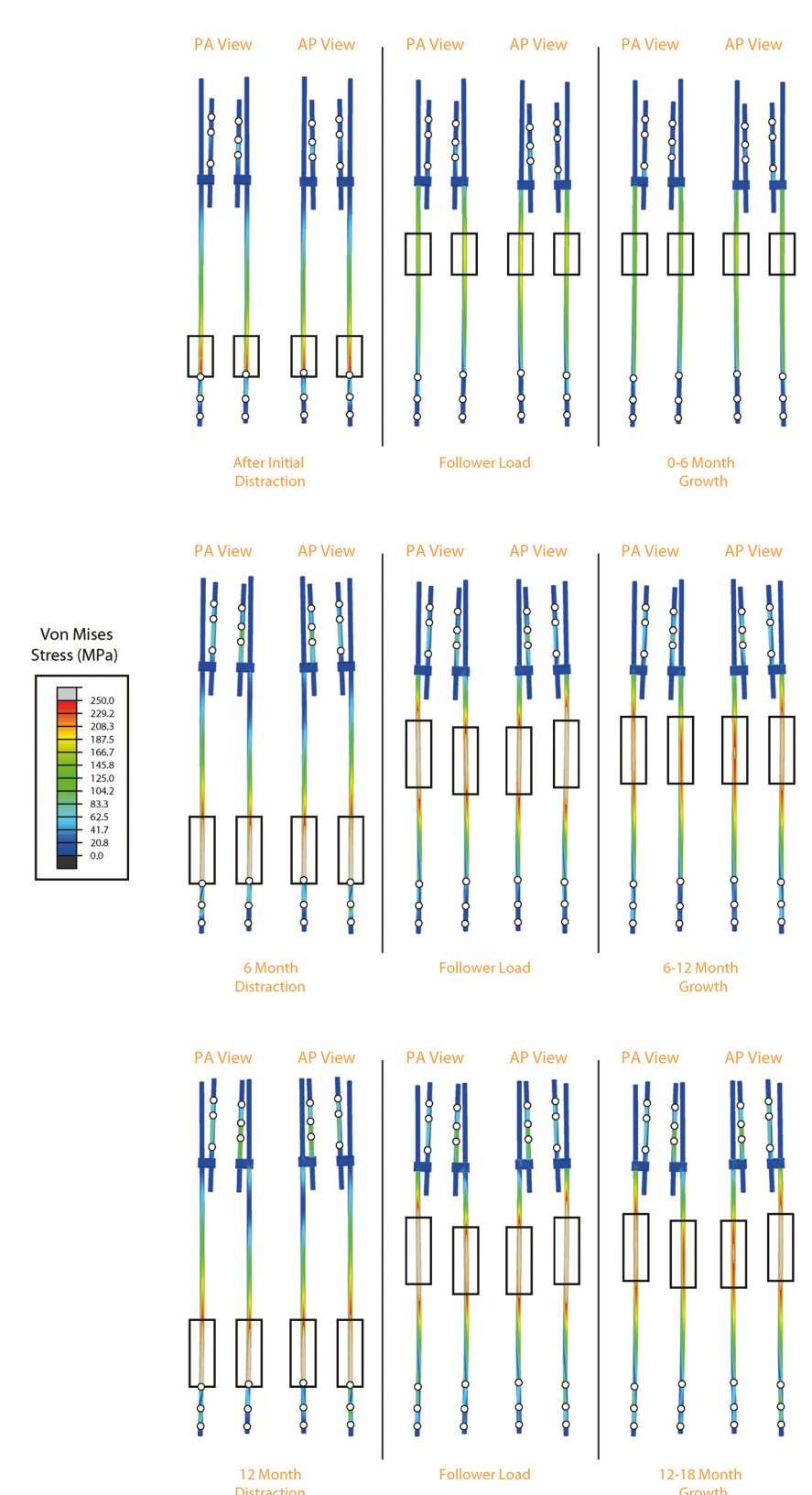


**Figure 7.** Von Mises stress plots in the Traditional Growing Rod model. Stress magnitude and locations in each rod are shown in the PA and AP positions. Changes over time are shown from top left to bottom right. The regions of high stress are outlined in black. AP indicates anterior-posterior; PA, posterior-anterior.

correction and higher T1-S1 growth compared to the SDS model. This continuously increasing curve correction in subsequent TGR lengthenings, however, contradicts clinical literature, where this phenomenon is rarely seen (when

excluding length gain during final fusion).<sup>31</sup> This discrepancy can be explained by the fact that the current FE model did not take into account the effect of spinal stiffening and autofusion that takes place when using forceful distractions.

E462 www.spinejournal.com May 2022

| TABLE 2. Spinal Morphology Over Time     |                              |       |       |  |  |
|--|------------------------------|-------|-------|--|--|
|  |                              | SDS   | TGR   |  |  |
| Main coronal Cobb angle ( <sup>O</sup> ) | Preoperative                 | 43.9  |       |  |  |
|  | Postoperative*               | 22.2  | 23.0  |  |  |
|  | 0-6 mo Growth <sup>†</sup>   | 23.2  | 28.3  |  |  |
|  | 6–12 mo Growth <sup>†</sup>  | 25.3  | 19.3  |  |  |
|  | 12-18 mo Growth <sup>†</sup> | 26.9  | 16.0  |  |  |
| T5-T12 kyphosis (°)                      | Preoperative                 | 25.1  |       |  |  |
|  | Postoperative*               | 19.9  | 20.0  |  |  |
|  | 0-6 mo Growth <sup>†</sup>   | 20.6  | 21.7  |  |  |
|  | 6–12 mo Growth <sup>†</sup>  | 21.5  | 18.9  |  |  |
|  | 12-18 mo Growth <sup>†</sup> | 22.7  | 16.6  |  |  |
| L1-S1 lordosis (°)                       | Preoperative                 | 49.0  |       |  |  |
|  | Postoperative*               | 47.4  | 48.2  |  |  |
|  | 0–6 mo Growth <sup>†</sup>   | 47.5  | 48.2  |  |  |
|  | 6–12 mo Growth <sup>†</sup>  | 48.3  | 47.6  |  |  |
|  | 12-18 mo Growth <sup>†</sup> | 48.9  | 47.4  |  |  |
| T1-S1 height, mm                         | Preoperative                 | 323.5 |       |  |  |
|  | Postoperative*               | 336.7 | 336.3 |  |  |
|  | 0–6 mo Growth <sup>†</sup>   | 340.7 | 338.2 |  |  |
|  | 6–12 mo Growth <sup>†</sup>  | 344.5 | 351.6 |  |  |
|  | 12-18 mo Growth <sup>†</sup> | 347.5 | 359.2 |  |  |

As the SDS and TGR model are the same until start of treatment, the preoperative values are identical for both implant systems.

 $<sup>^{\</sup>dagger}$ Represents the value at the end of the respective growth period (for TGR, this represents the value just before a distraction).

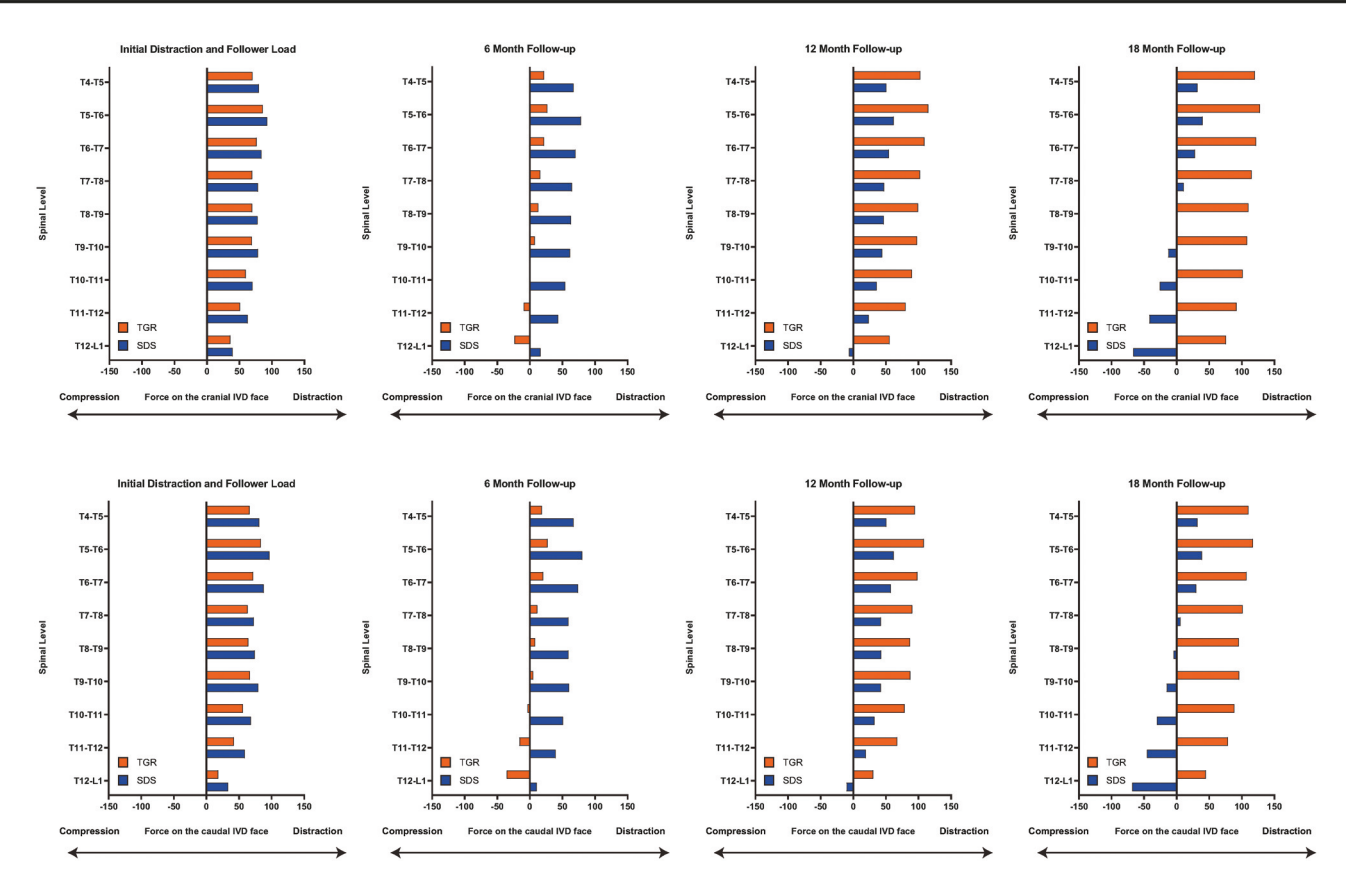


**Figure 8.** Forces on the intervertebral discs spanned by the construct. Normal forces on the upper IVD faces (top) and the lower IVD faces (bottom) extracted from the free-body diagrams. The evaluated IVDs were the ones spanned by the growing construct. Changes over time are shown from left to right. Positive forces denote distraction, negative forces denote compression. IVD indicates intervertebral disc; SDS, Spring Distraction System; TGR, traditional growing rod.

Spine www.spinejournal.com E463

<sup>\*</sup>After follower load introduction.

These have been linked to cause both the "law of diminishing returns" as well as the necessary increasing distraction forces in TGR treatment. <sup>32,33</sup> Ideally, a biofidelic model would include this effect. The present study did not attempt this for two reasons. First, it is unknown when, and to what extent, this stiffening occurs *in vivo* and in which structures and spinal levels it takes place. Second, it is yet unknown whether this effect also takes place in SDS patients, as these patients have relatively short follow-up. As this process is known to take place during TGR treatment, the outcomes reported in this manuscript thus represent a best-case scenario for the TGR model, as stiffening likely leads to reduced correction and spinal growth, and necessitates higher distraction forces which increase implant stresses further. <sup>16,23,24</sup>

As of yet, the SDS has been implanted in >70 patients as part of clinical studies. Two year follow-up results have shown that it was able to provide adequate curve correction that could be maintained at latest follow-up whilst providing T1-S1 growth exceeding 10 mm/year. 17,18 A recent complication analysis between SDS and (hybrid) MCGR patients showed that the SDS could not prevent rod fractures when 4.5 mm rods were used.<sup>34</sup> A review of these fractures showed similar points of failure to the locations highlighted by the present study. In several patients with bilateral springs, fractures occurred near the distal anchors, often close to the vicinity of the locking buttress, potentially due to set screw notches that act as stress concentrators.<sup>35</sup> These results of stress locations of growing rods are in line with recent studies on rod fractures and offer opportunities to prevent these complications. 11,25 Excessive rod bending in areas with high rod stress should be prevented (midconstruct for TGR, near the distal anchors for SDS), as this might introduce notches that weaken the rods. 36-38 Use of larger diameter rods may reduce overall rod stresses, although larger rods could mitigate these benefits by increasing construct stiffness, which has also been shown to be a risk factor for rod fractures. 39,40

The use of the SDS springs allows for increased loadsharing of the IVDs during periods of increased loading. Recent studies on "growth-friendly" implants have shown that IVDs within a distraction construct show a decrease in height and volume over time coincident with degenerative changes seen on MRI. <sup>20,21</sup> In the present model, the SDS IVDs were under more distraction during the first 6 months. However, this effect reversed after the first TGR distraction, with the spanned IVDs in the TGR model under increasing amounts of distraction, whereas the IVDs in the SDS model were increasingly subjected to compressive forces again. This confirms the hypothesis that over time, the SDS allows for increased IVD load-sharing. Whether this also results in less IVD degeneration is unknown and will require clinical validation using 3D imaging.

The present study investigated one SDS configuration with bilateral 75N springs. While this configuration is still commonly used (*e.g.*, for neuromuscular patients), for stiffer congenital or idiopathic curves, we now often combine a

100 N spring on the curve concavity with a sliding rod on the curve convexity (without a spring) that is fixated to the apex (for increased apical control). It is likely that this differential method of force application affects rod stress distribution, load-sharing of the spine, and spinal growth. Future FE studies should compare these new configurations to the present one to determine which one provides superior results with respect to curve correction and rod stress.

This is the first study investigating biomechanical differences between the TGR and the SDS. Strengths include the use of a previously validated, patient-specific, EOS FE model. In addition, representative modeling steps and implant configurations were modeled which ensured a fair comparison between both models. Limitations include the fact that several material properties had to be estimated from adult values and that certain effects such as spinal stiffening and autofusion were not present in the model. Future work will need to study how this phenomenon, in addition to different implant configurations, longer follow-up, and spinal motion affects implant biomechanics and spinal morphology.

#### CONCLUSION

During FE simulation of implantation and 18-month follow-up, several biomechanical and morphological differences were observed between TGR and SDS treatment. In the present models that did not model the effect of stiffening and autofusion of the spine, the additional TGR distractions resulted in better coronal curve correction and higher T1-S1 growth, but at the expense of increased stress-shielding of the IVD and increased propensity of rod fractures.

## **>Key Points**

- During finite element simulation of implantation and 18-month follow-up, several biomechanical and morphological differences were observed between TGR and SDS treatment.
- During each intermittent lengthening, TGR rod stress increased significantly, to levels much higher than those in SDS treatment.
- ☐ In the present models that did not model the effect of stiffening and autofusion of the spine, the additional TGR lenghtenings resulted in better coronal curve correction and higher T1-S1 growth compared to SDS.
- The intervertebral discs in the SDS model underwent much less-stress-shielding than those in the TGR model.

#### Acknowledgments

We would like to acknowledge the NSF-IUCRC center (CDMI) at the University of Toledo, Ohio State University, and the University of California-San Francisco for supporting this study in part.

#### References

- Skaggs DL, Akbarnia BA, Flynn JM, et al. A classification of growth friendly spine implants. J Pediatr Orthop 2014;34:260–74.
- 2. Akbarnia BA, Marks DS, Boachie-Adjei O, et al. Dual growing rod technique for the treatment of progressive early-onset scoliosis. *Spine (Phila Pa 1976)* 2005;30 (suppl):S46–57.
- US Food and Drug Administration. FDA Drug Safety Communication: FDA review results in new warnings about using general anesthetics and sedation drugs in young children and pregnant women. 2017.
- 4. Bess S, Akbarnia BA, Thompson GH, et al. Complications of growing-rod treatment for early-onset scoliosis: Analysis of one hundred and forty patients. *J Bone Jt Surg A* 2010;92:2533–43.
- 5. Sankar WN, Skaggs DL, Yazici M, et al. Lengthening of dual growing rods and the law of diminishing returns. *Spine (Phila Pa 1976)* 2011;36:806–9.
- 6. Ahmad A, Subramanian T, Wilson-Macdonald J, et al. Quantifying the 'law of diminishing returns' in magnetically controlled growing rods. *Bone Jt J* 2017;99B:1658–64.
- 7. Agarwal A, Goswami A, Vijayaraghavan GP, et al. Quantitative characteristics of consecutive lengthening episodes in early-onset scoliosis (EOS) patients with dual growth rods. *Spine (Phila Pa 1976)* 2019;44:397–403.
- 8. Noordeen HM, Shah SA, Elsebaie HB, et al. In vivo distraction force and length measurements of growing rods: Which factors influence the ability to lengthen?. *Spine (Phila Pa 1976)* 2011;36:2299–303.
- Thakar C, Kieser DC, Mardare M, et al. Systematic review of the complications associated with magnetically controlled growing rods for the treatment of early onset scoliosis. *Eur Spine J* 2018;27:2062–71.
- Choi E, Yaszay B, Mundis G, et al. Implant complications after magnetically controlled growing rods for early onset scoliosis. *J Pediatr Orthop* 2017;37:e588–92.
- 11. Hill G, Nagaraja S, Akbarnia BA, et al. Retrieval and clinical analysis of distraction-based dual growing rod constructs for early-onset scoliosis. *Spine J* 2017;17:1506–18.
- 12. Joyce TJ, Smith SL, Rushton PRP, et al. Analysis of explanted magnetically controlled growing rods from seven UK spinal centers. *Spine (Phila Pa 1976)* 2018;43:E16–22.
- 13. Agarwal A, Kelkar A, Agarwal AG, et al. Device-related complications associated with magec rod usage for distraction-based correction of scoliosis. *Spine Surg Relat Res* 2020;4:148–51.
- 14. Cahill PJ, Marvil S, Cuddihy L, et al. Autofusion in the immature spine treated with growing rods. *Spine (Phila Pa 1976)* 2014;35: E1199–203.
- 15. Agarwal A, Agarwal AK, Jayaswal A, et al. Smaller interval distractions may reduce chances of growth rod breakage without impeding desired spinal growth: a finite element study. *Spine Deform* 2014;2:430–6.
- 16. Agarwal A, Jayaswal A, Goel VK, et al. Patient-specific distraction regimen to avoid growth-rod failure. *Spine (Phila Pa 1976)* 2018;43:E221-6.
- 17. Wijdicks SPJ, Lemans JVC, Verkerke GJ, et al. The potential of spring distraction to dynamically correct complex spinal deformities in the growing child. *Eur Spine J* 2021;30:714–23.
- 18. Lemans JVC, Wijdicks SPJ, Castelein RM, et al. Spring distraction system for dynamic growth guidance of early onset scoliosis: 2 year prospective follow-up of 24 patients. *Spine J* 2021;21:671–81.
- 19. Myers MA, Casciani T, Whitbeck GMJ, et al. Vertebral body osteopenia associated with posterolateral spine fusion in humans. *Spine (Phila Pa 1976)* 1996;21:2368–71.
- Rong T, Shen J, Kwan K, et al. Vertebral growth around distal instrumented vertebra in patients with early-onset scoliosis who underwent traditional dual growing rod treatment. Spine (Phila Pa 1976) 2019;44:855–65.

- 21. Lippross S, Girmond P, Lüders KA, et al. Smaller intervertebral disc volume and more disc degeneration after spinal distraction in scoliotic children. *J Clin Med* 2021;10:; doi:10.3390/jcm10102124.
- 22. Agarwal A, Agarwal AK, Jayaswal A, et al. Effect of distraction force on growth and biomechanics of the spine: A finite element study on normal juvenile spine with dual growth rod instrumentation. *Spine Deform* 2014;2:260–9.
- 23. Agarwal A, Zakeri A, Agarwal AK, et al. Distraction magnitude and frequency affects the outcome in juvenile idiopathic patients with growth rods: Finite element study using a representative scoliotic spine model. *Spine J* 2015;15:Error: FPage (1848) is higher than LPage (855)!.
- 24. Agarwal A, Agarwal AK, Jayaswal A, et al. Outcomes of optimal distraction forces and frequencies in growth rod surgery for different types of scoliotic curves: an in silico and in vitro study. Spine Deform 2017;5:18–26.
- 25. Agarwal A, Kodigudla M, Kelkar A, et al. Towards a validated patient-specific computational modeling framework to identify failure regions in traditional growing rods in patients with early onset scoliosis. *North Am Spine Soc J* 2021;5:1000432.
- 26. Schultz A, Andersson GB, Ortengren R, et al. Analysis and quantitative myoelectric measurements of loads on the lumbar spine when holding weights in standing postures. *Spine (Phila Pa 1976)* 1982;7:390–7.
- 27. Agarwal A. Mitigating biomechanical complications of growth rods in juvenile idiopathic scoliosis. Published online 2015. Available at: http://rave.ohiolink.edu/etdc/view?acc\_num=toledo1429875994.
- 28. Shi L, Wang D, Driscoll M, et al. Biomechanical analysis and modeling of different vertebral growth patterns in adolescent idiopathic scoliosis and healthy subjects. *Scoliosis* 2011;6:1–8.
- 29. Stokes IAF, Windisch L. Vertebral height growth predominates over intervertebral disc height growth in adolescents with scoliosis. *Spine (Phila Pa 1976)* 2006;31:1600–4.
- 30. Fok J, Adeeb S, Carey J. FEM simulation of non-progressive growth from asymmetric loading and vicious cycle theory: scoliosis study proof of concept. *Open Biomed Eng J* 2010;4:162–9.
- 31. Wijdicks SPJ, Tromp IN, Yazici M, et al. A comparison of growth among growth-friendly systems for scoliosis: a systematic review. *Spine J* 2019;19:789–99.
- 32. Agarwal A. Biomechanics of Surgical Intervention Associated with Early-Onset Scoliosis A comparison of growth among growth-friendly systems for scoliosis: a systematic review. *Early-Onset Scoliosis CRC Press* 2021;93–106.
- 33. Ahmad AA. Early onset scoliosis and current treatment methods. *J Clin Orthop trauma* 2020;11:184–90.
- 34. Lemans JVC, Tabeling CS, Castelein RM, et al. Identifying complications and failure modes of innovative growing rod configurations using the (hybrid) magnetically controlled growing rod and the spring distraction system. *Spine Deform* 2021;9:1679–89.
- 35. Dick JC, Bourgeault CA. Notch sensitivity of titanium alloy, commercially pure titanium, and stainless steel spinal implants. *Spine (Phila Pa 1976)* 2001;26:1668–72.
- 36. Demura S, Murakami H, Hayashi H, et al. Influence of rod contouring on rod strength and stiffness in spine surgery. *Orthopedics* 2015;38:e520-3.
- 37. Slivka MA, Fan YK, Eck JC. The effect of contouring on fatigue strength of spinal rods: is it okay to re-bend and which materials are best?. *Spine Deform* 2013;1:395–400.
- 38. Lindsey C, Deviren V, Xu Z, et al. The effects of rod contouring on spinal construct fatigue strength. *Spine (Phila Pa 1976)* 2006;31: 1680–7.
- 39. Yang JS, Sponseller PD, Thompson GH, et al. Growing rod fractures: Risk factors and opportunities for prevention. *Spine* (*Phila Pa* 1976) 2011;36:1639–44.
- 40. Hill G, Nagaraja S, Bridges A, et al. Mechanical performance of traditional distraction-based dual growing rod constructs. *Spine J* 2019;19:744–54.

Spine www.spinejournal.com **E465**